

Experimental report

18/03/2020

Proposal: 7-03-181

Council: 4/2019

Title: Dynamics of the formamidinium organic cation in mixed hybrid inorganic-organic perovskites

Research area: Materials

This proposal is a continuation of 7-03-169

Main proposer: Rasmus LAVEN

Experimental team: Rasmus LAVEN
Adrien PERRICHON

Local contacts: Michael Marek KOZA
Markus APPEL

Samples: MA_{1-x}FA_xPbI₃

Instrument	Requested days	Allocated days	From	To
IN5	4	3	13/09/2019	16/09/2019
IN16B	11	5	05/09/2019	10/09/2019

Abstract:

The aim of this continuation proposal is to provide a detailed characterization of the local dynamics of the formamidinium organic cation in the mixed hybrid inorganic-organic perovskites MA_{1-x}FA_xPbI₃ (MA = methylammonium, CH₃NH₃; FA = formamidinium, CH(NH₂)₂). To complement our previous experiment, we here propose to use IN16B in order to probe the dynamics in the low temperature phases, as well as to measure on N-deuterated FAPbI₃ at IN5 in order to discriminate between the different rotational contributions of FA. The results will be linked to structural studies by diffraction techniques in order to provide a detailed understanding of the FA dynamics over a wide temperature range.

Dynamics of the formamidinium organic cation in mixed hybrid inorganic-organic perovskites (exp. 7-03-181)

1 Scientific background

Hybrid inorganic-organic perovskites have attracted an enormous interest recently due to their promising applications as absorbers in photovoltaic devices [1, 2]. One of the most promising materials has the chemical formula $\text{MA}_{1-x}\text{FA}_x\text{PbI}_3$, where MA is methylammonium, CH_3NH_3 , and FA is formamidinium, $\text{CH}(\text{NH}_2)_2^+$. An important question with respect to $\text{MA}_{1-x}\text{FA}_x\text{PbI}_3$ concerns the role the organic cation (MA and FA) has on the performance of the perovskite solar cell. The organic cation has been hypothesized to affect several properties including, e.g., the formation of microscopic (anti)ferroelectric domains, which helps to separate charge carriers by the electric field and therefore results in longer carrier diffusion lengths [3], and a giant modulation of the dielectric function which, in turn, lowers the exciton binding energy [4]. Still, these effects are currently under debate and some studies are contradictory to each other. It is therefore important to gain a full understanding of the dynamics of the organic cation at the atomic scale. A well-suited method for this is quasielastic neutron scattering (QENS), since hydrogen has a very large incoherent cross section for neutrons; therefore, the QENS signal will be dominated by contributions from the hydrogen atoms in the MA or FA molecule, and the organic cation dynamics can be probed. As the majority of previous studies have focused on MAPbI_3 [3, 4], we aimed to elucidate the dynamics of the FA organic cation in the mixed hybrid inorganic-organic perovskites $\text{MA}_{1-x}\text{FA}_x\text{PbI}_3$ by employing QENS.

2 Experimental details

The QENS experiments were performed at IN16b and IN5. Powder samples of $\text{MA}_{1-x}\text{FA}_x\text{PbI}_3$ ($x = 0.0, 0.6, 0.9, \text{ and } 1.0$) were filled inside annular aluminium cans. FAPbI_3 was annealed *ex-situ* at 165°C for 2 hours directly prior to the measurements to form the metastable cubic phase [5, 6]. The measurements on IN5 were performed with both 5 \AA and 2.5 \AA incident neutron wavelengths. For 2.5 \AA neutrons, an energy resolution of 0.1 meV and accessible q -range of $\sim 0.1 - 2.1 \text{ \AA}^{-1}$ were obtained, whilst for 5 \AA neutrons the respective values were 0.62 meV and $\sim 0.1 - 4.1 \text{ \AA}^{-1}$. The measurements were performed in the temperature range $2 - 350 \text{ K}$. At IN5, the samples with $x = 0.0, 0.9, \text{ and } 1.0$ were measured. Standard corrections were applied to the time-of-flight data with the LAMP software [7] and included normalization to a vanadium standard, subtraction of an empty can measurement, correction for the energy-dependent efficiency of the detectors, and suppression of some "blind" or noisy detectors. The measured cross-section was converted to the (q, E) domain to obtain the measured dynamical structure factor $S(q, E)$. Measurements of the sample at 2 K was used as a resolution function in the fitting of the quasielastic lineshape. In addition, the generalized phonon density of states (GDOS) was calculated from the experimental data in order to study the low-energy vibrational modes as a function of temperature. At IN16b, an incident wavelength of 3.275 \AA was used. Using the Si(311) crystal analysers, an energy resolution of $\sim 2 \mu\text{eV}$ and an accessible q -range of $1.5 - 3.5 \text{ \AA}^{-1}$, were obtained. The measurements were performed in the temperature range $2 - 200 \text{ K}$. At IN16b, samples with $x = 0.0, 0.6, \text{ and } 1.0$ were measured. Standard data corrections were performed using Mantid [8], and included normalisation to a Vanadium standard (for detector efficiencies), background subtraction and self absorption corrections.

3 Preliminary results

The following section showcase some of the results which we obtained at IN16b. The experiment at IN16b was started by performing an elastic window scan as a function of temperature. During that measurement we measured both the elastic intensity and the inelastic intensities at energy transfers of $4 \mu\text{eV}$ and $10 \mu\text{eV}$. Some of these results are shown in Fig. 1 (a)-(b). Fig. 1 (a) shows the elastic intensity of the three measured samples ($\text{MA}_{1-x}\text{FA}_x\text{PbI}_3$, $x = 0.0, 0.6, \text{ and } 1.0$). For FAPbI_3 , a drastic change in slope

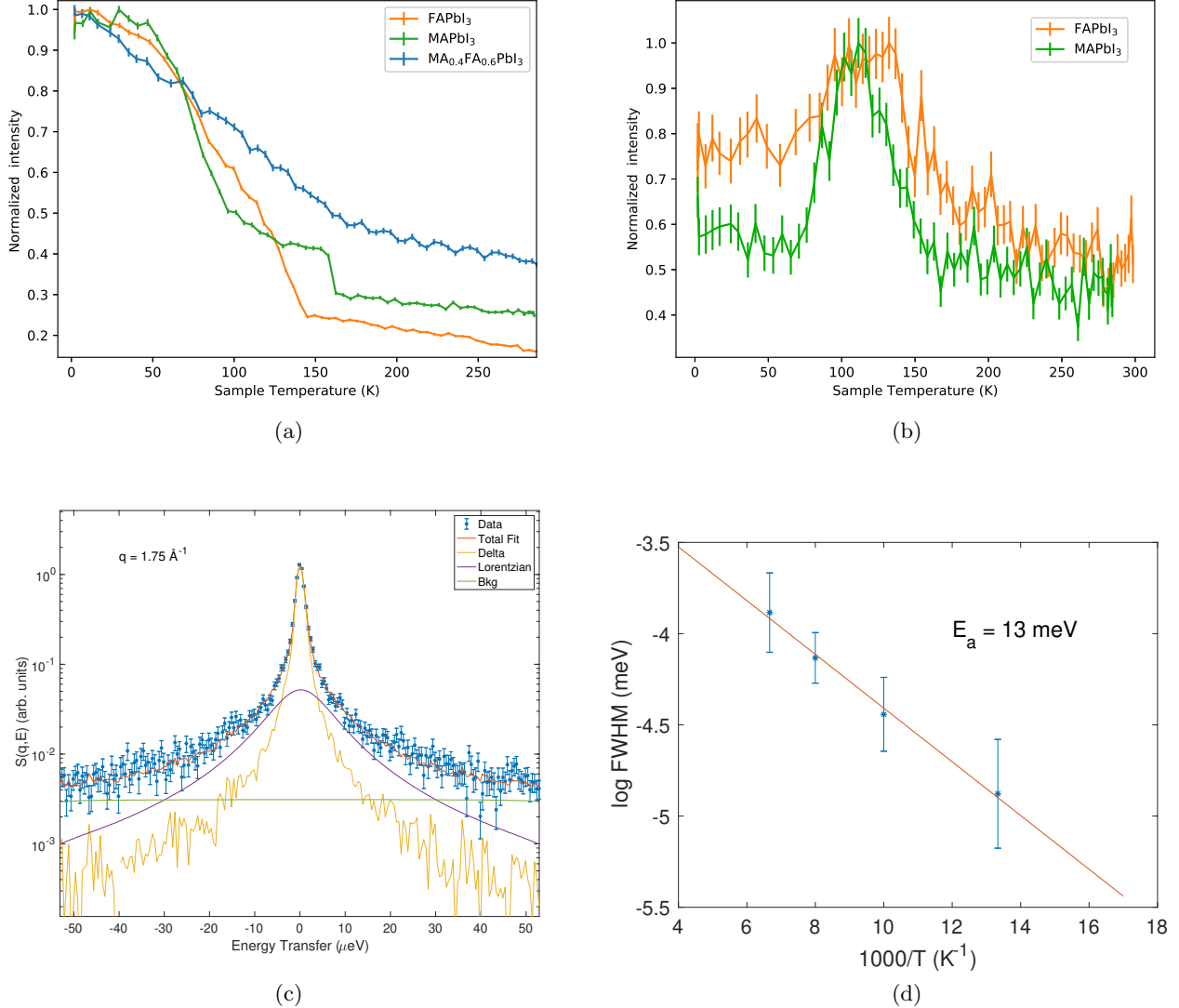


Figure 1: (a) Elastic fixed window scan for the three samples as measured upon cooling from room temperature to 2 K. (b) Inelastic fixed window scan of FAPbI₃ and MAPbI₃ measured at $E = 10 \mu\text{eV}$ upon cooling from room temperature to 2 K. (c) Example fitting to the quasielastic lineshape of FAPbI₃ at $T = 125 \text{ K}$ and $q = 1.75 \text{ \AA}^{-1}$. (d) Arrhenius plot of the obtained quasielastic linewidth (FWHM). An activation energy of about 13 meV was extracted.

is seen around 145 K, where the elastic intensity starts to increase much faster upon cooling further. This temperature corresponds well to the phase transition of FAPbI₃ from the tetragonal β -phase, into the disordered low-temperature γ -phase [9]. Thus, this indicates that the re-orientational dynamics of FA is too fast to be probed at IN16b in the tetragonal and cubic phase, while upon entering the low-temperature γ -phase, the FA cation dynamics is drastically slowed down and can be probed at IN16b. For MAPbI₃, a discontinuity in the elastic intensity is seen around 162 K, which corresponds to the tetragonal-orthorhombic phase transition. Also the MA reorientations in MAPbI₃ is too fast to be observed at IN16b in the tetragonal and cubic phases. The MA_{0.4}FA_{0.6}PbI₃ sample shows, in great contrast to the pure stoichiometric samples, a more smooth temperature dependence, with no large features over the probed temperature range. This indicates that the temperature dependence of the cation dynamics is greatly different for the mixed stoichiometries, and is partly explained by the lack of phase transitions in the low-temperature regime. The inelastic intensities at $10 \mu\text{eV}$ as function of sample temperature are shown in Fig. 1 (b) for FAPbI₃ and MAPbI₃. For MAPbI₃ a clear and well-defined peak is seen between 75 – 160

K. This is indicative of a single quasielastic component within the probed dynamics range, which in this case corresponds to the three-fold methyl and/or ammonia rotations around the C – N axis, in accordance with previous QENS studies on MAPbI₃ [3, 4]. For FAPbI₃ a much broader and less well-defined peak is seen between 55 – 175 K. This cannot be satisfactorily be fitted to an expression containing a single quasielastic component, thus pointing towards a more complicated FA dynamics in the low temperature phase as compared to MAPbI₃. This is rationalized by the fact that the low temperature phase of FAPbI₃ is believed to be locally disordered [9]. Even though the quasielastic scattering of the low-temperature phase of FAPbI₃ most likely contains many components with similar relaxational times, this is difficult to separate out experimentally when fitting the quasielastic lineshape. The quasielastic lineshape of FAPbI₃ were well modelled by a single Lorentzian function for all measured temperatures, as is shown in Fig. 1 (c) for $T = 150$ K. The temperature dependence of the linewidth of this Lorentzian was used to derive an activation energy of about 13 meV (c.f. Fig. 1 (d)).

References

- [1] W. S. Yang, N. J. J. Jun Hong Noh, Y. C. Kim, S. Ryu, J. Seo, and S. I. Seok, “High-performance photovoltaic perovskite layers fabricated through intramolecular exchange,” *Science (80-.)*, vol. 348, no. 111, pp. 2013–2017, 2015.
- [2] J. P. Correa-Baena, A. Abate, M. Saliba, W. Tress, T. Jesper Jacobsson, M. Grätzel, and A. Hagfeldt, “The rapid evolution of highly efficient perovskite solar cells,” *Energy Environ. Sci.*, vol. 10, no. 3, pp. 710–727, 2017.
- [3] A. M. Leguy, J. M. Frost, A. P. McMahon, V. G. Sakai, W. Kochelmann, C. Law, X. Li, F. Foglia, A. Walsh, B. C. O’Regan, J. Nelson, J. T. Cabral, and P. R. Barnes, “The dynamics of methylammonium ions in hybrid organic-inorganic perovskite solar cells,” *Nat. Commun.*, vol. 6, no. May, 2015.
- [4] T. Chen, B. J. Foley, B. Ipek, M. Tyagi, J. R. D. Copley, C. M. Brown, J. J. Choi, and S.-H. Lee, “Rotational dynamics of organic cations in the CH₃NH₃PbI₃ perovskite,” *Phys. Chem. Chem. Phys.*, vol. 17, no. 46, pp. 31278–31286, 2015.
- [5] A. A. Zhumekenov, M. I. Saidaminov, A. Haque, E. Alarousu, S. P. Sarmah, B. Murali, I. Dursun, X.-h. Miao, A. L. Abdelhady, T. Wu, O. F. Mohammed, and O. M. Bakr, “Formamidinium Lead Halide Perovskite Crystals with Unprecedented Long Carrier Dynamics and Diffusion Length,” pp. 1–7, 2016.
- [6] A. Pisanu, C. Ferrara, P. Quadrelli, G. Guizzetti, M. Patrini, C. Milanese, C. Tealdi, and L. Malavasi, “The FA_{1-x}MA_xPbI₃ System: Correlations among Stoichiometry Control, Crystal Structure, Optical Properties, and Phase Stability,” *J. Phys. Chem. C*, vol. 121, no. 16, pp. 8746–8751, 2017.
- [7] D. Richard, M. Ferrand, and G. J. Kearley, “Analysis and visualisation of neutron-scattering data,” *J. Neutron Res.*, vol. 4, no. 1-4, pp. 33–39, 1996.
- [8] O. Arnold, J. C. Bilheux, J. M. Borreguero, A. Buts, S. I. Campbell, L. Chapon, M. Doucet, N. Draper, R. Ferraz Leal, M. A. Gigg, V. E. Lynch, A. Markvardsen, D. J. Mikkelsen, R. L. Mikkelsen, R. Miller, K. Palmen, P. Parker, G. Passos, T. G. Perring, P. F. Peterson, S. Ren, M. A. Reuter, A. T. Savici, J. W. Taylor, R. J. Taylor, R. Tolchenov, W. Zhou, and J. Zikovsky, “Mantid - Data analysis and visualization package for neutron scattering and μ SR experiments,” *Nucl. Instruments Methods Phys. Res. Sect. A Accel. Spectrometers, Detect. Assoc. Equip.*, vol. 764, pp. 156–166, 2014.
- [9] O. J. Weber, D. Ghosh, S. Gaines, P. F. Henry, A. B. Walker, M. S. Islam, and M. T. Weller, “Phase Behavior and Polymorphism of Formamidinium Lead Iodide,” *Chem. Mater.*, vol. 30, no. 11, pp. 3768–3778, 2018.